

# A Highly Efficient Photocatalytic System for Hydrogen Production by a Robust Hydrogenase Mimic in an Aqueous Solution\*\*

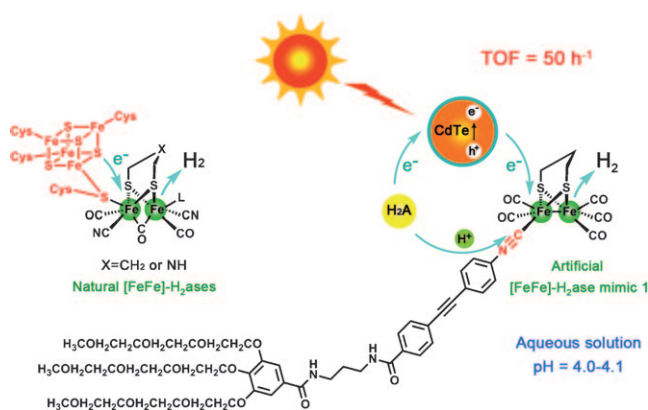
Feng Wang, Wen-Guang Wang, Xiao-Jun Wang, Hong-Yan Wang, Chen-Ho Tung, and Li-Zhu Wu\*

Utilization of sunlight to make solar fuels represents a promising solution to the looming energy crisis and climate change. Hydrogen ( $H_2$ ), with high specific enthalpy of combustion and benign combustion product (water), is envisaged to be the ideal fuel for reducing mankind's dependence on fossil fuels and subsequent emissions of greenhouse gases.<sup>[1,2]</sup> Long ago, nature figured out how to use a photosynthetic complex to capture sunlight, and then to store its energy in a chemical form,  $H_2$ , in which hydrogenases ( $H_2$ ases) can catalyze the reversible reduction of protons to  $H_2$  with remarkable activity.<sup>[3]</sup> With the structural elucidation of [FeFe]- $H_2$ ases (Scheme 1),<sup>[4,5]</sup> scientists are working hard to develop artificial photosynthetic systems using [FeFe]- $H_2$ ases mimics for  $H_2$  generation,<sup>[6–10]</sup> multicomponent systems,<sup>[11–13]</sup>

covalently linked dyads,<sup>[14–19]</sup> and supramolecular assemblies.<sup>[20–22]</sup> However, in comparison to the efficient [FeFe]- $H_2$ ases in nature, these systems thus far give rise to none or a small amount of  $H_2$  upon irradiation, and finally finish their photochemical  $H_2$  production in organic solutions or a mixture of organic solvents and water. More strikingly, these synthetic [FeFe]- $H_2$ ases mimics are not stable and would decompose generally within 1 hour of irradiation. Thus the creation of an artificial [FeFe]- $H_2$ ase system that can produce  $H_2$  by visible light with high catalytic activity and stability in an aqueous solution remains a significant basic science challenge.

Herein, we report a highly efficient photocatalytic system that is comprised of an artificial water-soluble [FeFe]- $H_2$ ase mimic **1**, photosensitizer, and ascorbic acid ( $H_2A$ ) for  $H_2$  production in pure water at room temperature (Scheme 1). Here, a cyanide (CN) group was incorporated to anchor three hydrophilic ether chains to the active site of the [FeFe]- $H_2$ ase mimic to enhance the solubility of catalyst **1** in water. Nanocrystal quantum dots, CdTe, stabilized by 3-mercaptopropionic acid (MPA–CdTe) was selected as the photosensitizer owing to its broad visible-light absorption, aqueous dispersion, and economical advantage over precious metal photosensitizers.<sup>[22,23]</sup> The  $H_2A$  served as a proton source and a sacrificial electron donor is water-soluble and thus allows for the incorporation of a large amount of  $H_2A$  in the reaction vessel. With this system, we are able to achieve the production of 786  $\mu\text{mol}$  (17.6 mL)  $H_2$  after 10 hours of irradiation ( $\lambda > 400\text{ nm}$ ) in pure water with turnover number (TON) and turnover frequency values (TOF) of up to 505 and 50  $\text{h}^{-1}$  under optimized conditions, which is, to the best of our knowledge, the highest photocatalytic efficiency and stability of artificial [FeFe]- $H_2$ ase catalysts obtained so far. Spectroscopic study and a light-driven  $H_2$  evolution experiment indicate that photoinduced electron transfer takes place from the MPA–CdTe species to [FeFe]- $H_2$ ase catalyst **1**. The  $H_2A$  is not only a proton source for  $H_2$  production but also an effective sacrificial electron donor for the hole formed in the MPA–CdTe after electron transfer. As a result a robust, efficient, and inexpensive system for the photocatalytic production of  $H_2$  based on an artificial [FeFe]- $H_2$ ase mimic in an aqueous solution is established.

The MPA–CdTe species were prepared according to the reported procedures and used directly.<sup>[24–26]</sup> On the basis of the low-energy absorption band centered at 571 nm, the particle size of the MPA–CdTe species was determined to be 3.4 nm using the equation developed by Peng and co-workers (see the Supporting Information).<sup>[27]</sup> For the [FeFe]- $H_2$ ase mimic **1**, the diiron core tethered to 4-(4-alkynyl-benzoic



**Scheme 1.** The structure of natural [FeFe]- $H_2$ ases and artificial [FeFe]- $H_2$ ase mimic **1**.

[\*] F. Wang, Dr. W.-G. Wang, X.-J. Wang, H.-Y. Wang, Prof. Dr. C.-H. Tung, Prof. Dr. L.-Z. Wu  
Key Laboratory of Photochemical Conversion and Optoelectronic Materials  
Technical Institute of Physics and Chemistry & Graduate University  
the Chinese Academy of Sciences, Beijing 100190 (P.R. China)  
Fax: (+86) 10-8254-3580  
E-mail: lzwu@mail.ipc.ac.cn

[\*\*] We are grateful for financial support from the Solar Energy Initiative of the Knowledge Innovation Program of the Chinese Academy of Sciences (KGCXZ-YW-389), the National Science Foundation of China (20732007, 21090343 and 50973125), the Ministry of Science and Technology of China (2007CB808004, 2007CB936001, and 2009CB22008), and the Bureau for Basic Research of the Chinese Academy of Sciences.

Supporting information for this article is available on the WWW under <http://dx.doi.org/10.1002/anie.201006352>.

acid)phenylisocyanide was firstly synthesized by the Sonogashira reaction of a [FeFe]-H<sub>2</sub>ase complex with 4-iodophenylisocyanide and 4-ethynylbenzoic acid in a yield of 75 %. This species was condensed with an amine bearing three hydrophilic ether chains to afford the desired catalyst **1** (52 %), which was well-characterized by <sup>1</sup>H NMR spectroscopy, mass spectrometry, and elemental analysis (see the Supporting Information). Of particular importance is that the [FeFe]-H<sub>2</sub>ase mimic **1** is quite soluble in pure water as expected.

The photochemical H<sub>2</sub> evolution experiments were carried out in 10 mL of water in the presence of the [FeFe]-H<sub>2</sub>ase mimic **1** ( $1.56 \times 10^{-4}$  M), MPA-CdTe ( $5.00 \times 10^{-4}$  M) (here and elsewhere, referring to the concentration of Cd<sup>2+</sup>), and H<sub>2</sub>A ( $8.52 \times 10^{-3}$  M, 15 mg) at room temperature under visible light ( $\lambda > 400$  nm). Because the MPA-capped CdTe species is very sensitive to the pH value of the solution,<sup>[28,29]</sup> we kept the initial concentration of H<sub>2</sub>A at 15 mg/10 mL with a pH value approximately equal to its pK<sub>a</sub> value of 4.03.<sup>[30]</sup> The reaction solution was placed in a Pyrex tube and then irradiated by a high-pressure Hanovia mercury lamp (500 W). A glass filter was used to cut off light below 400 nm to guarantee the irradiation by visible light. The generated photoproduct of H<sub>2</sub> was characterized by GC analysis using a molecular sieve column (5 Å), thermal conductivity detector, and nitrogen carrier gas with methane as the internal standard. The response factor of 2.76 for H<sub>2</sub>/CH<sub>4</sub> was determined by calibration with known amounts of H<sub>2</sub> and CH<sub>4</sub> under the experimental conditions. Figure 1a (triangle) shows the H<sub>2</sub> production over time from the mixture under irradiation. The rate of H<sub>2</sub> production was noted as linear during the first 6 hours, and then gradually declined over the next 2 hours. Irrespective of H<sub>2</sub> dissolution in the solvent, the amount of H<sub>2</sub> reached 58 μmol (1.3 mL) within 8 hours of irradiation. Control experiments indicated that the MPA-CdTe species, [FeFe]-H<sub>2</sub>ase mimic **1**, H<sub>2</sub>A, and light are all essential for H<sub>2</sub> generation; the absence of any of them yielded unobservable to insignificant amount of H<sub>2</sub> (Figure S1 in the Supporting Information).

The rate of light-driven H<sub>2</sub> production was found to depend on the pH value of the solution, the concentration of H<sub>2</sub>A, and the MPA-CdTe species. As a proton source, the amount of H<sub>2</sub>A affects the pH value of the aqueous solution. To ensure the same concentration of H<sub>2</sub>A throughout the experiment, we adjusted the pH value with HCl and NaOH prior to irradiation. As shown in Figure 1b, a sharp maximal rate for H<sub>2</sub> generation was observed at pH 4.0, while significant amounts of H<sub>2</sub> were also obtained at either lower or higher pH values. This pH-dependent effect is related to a number of factors, including the equilibrium of H<sub>2</sub>A ↔ H<sup>+</sup> + HA<sup>-</sup>, a change in the H<sup>+</sup>/H<sub>2</sub> reduction potential of the [FeFe]-H<sub>2</sub>ase mimic **1** and stability of the MPA-CdTe species. At higher pH, for example, the decrease in the rate of H<sub>2</sub> generation is likely a result of unfavorable protonation of the reduced [FeFe]-H<sub>2</sub>ase mimic **1**, whereas at lower pH values, the MPA ligands would dissociate from the CdTe surface causing precipitation and defects that can capture the excited electrons on the surface of the MPA-CdTe species.<sup>[28,29]</sup> Simultaneously, the equilibrium of H<sub>2</sub>A to HA<sup>-</sup> and H<sup>+</sup> is suppressed, thus lowering the ability of H<sub>2</sub>A to function as a

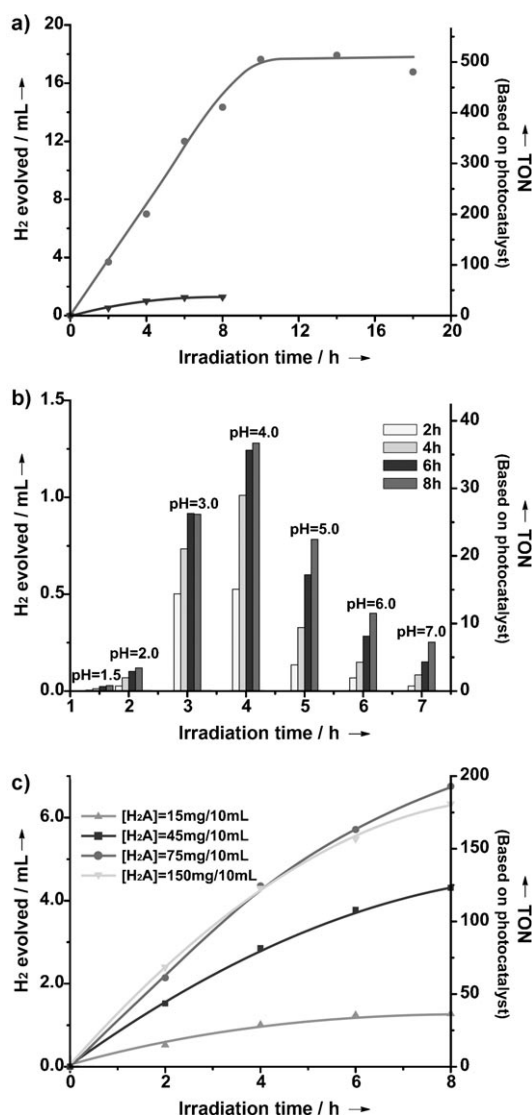


**Figure 1.** a) Photocatalytic H<sub>2</sub> evolution at pH 4.0–4.1 in H<sub>2</sub>O; sample concentration: [FeFe]-H<sub>2</sub>ase mimic **1** ( $1.56 \times 10^{-4}$  M), H<sub>2</sub>A ( $8.52 \times 10^{-3}$  M), MPA-CdTe ( $5.00 \times 10^{-4}$  M); triangle); [FeFe]-H<sub>2</sub>ase mimic **1** ( $1.56 \times 10^{-4}$  M), H<sub>2</sub>A ( $8.52 \times 10^{-3}$  M), MPA-CdTe ( $1.00 \times 10^{-3}$  M); circle); b) Photocatalytic H<sub>2</sub> evolution in H<sub>2</sub>O at different pH values; [FeFe]-H<sub>2</sub>ase mimic **1** ( $1.56 \times 10^{-4}$  M), MPA-CdTe ( $5.00 \times 10^{-4}$  M), H<sub>2</sub>A ( $8.52 \times 10^{-3}$  M); c) Photocatalytic H<sub>2</sub> evolution at pH 4.0–4.1 in H<sub>2</sub>O as a function of H<sub>2</sub>A concentration; [FeFe]-H<sub>2</sub>ase mimic **1** ( $1.56 \times 10^{-4}$  M), MPA-CdTe ( $5.00 \times 10^{-4}$  M), H<sub>2</sub>A ( $8.52 \times 10^{-3}$  M– $8.52 \times 10^{-2}$  M), respectively.

sacrificial electron donor. This behavior is well manifested by the fact that at the optimal pH value of 4.0, a significant improvement in H<sub>2</sub> production was observed when the concentration of H<sub>2</sub>A was increased from 15 mg/10 mL to 75 mg/10 mL (Figure 1c). Further increasing the concentration of H<sub>2</sub>A to 150 mg/10 mL led to no further increase in H<sub>2</sub> production. Clearly, H<sub>2</sub>A is crucial for photocatalytic H<sub>2</sub> production. The concentration of the MPA-CdTe also affects the rate of light-driven H<sub>2</sub> production. When the concentration of the MPA-CdTe species was increased from  $1.60 \times 10^{-4}$  M to  $5.00 \times 10^{-4}$  M in the solution at pH 4.0, where H<sub>2</sub>A is 15 mg/10 mL, the rate of H<sub>2</sub> production was much improved

(Figure S2). Taken together, we carried out the experiment under optimized conditions. A total of 786  $\mu\text{mol}$  (17.6 mL)  $\text{H}_2$  was produced from an aqueous solution containing [FeFe]- $\text{H}_2$ ase catalyst **1** ( $1.56 \times 10^{-4} \text{ M}$ ), MPA-CdTe ( $1.00 \times 10^{-3} \text{ M}$ ), and  $\text{H}_2\text{A}$  ( $8.52 \times 10^{-2} \text{ M}$ , 150 mg/10 mL) at pH 4.0. As shown in Figure 1a (circle), the production of more than 500 equivalents of  $\text{H}_2$  per [FeFe]- $\text{H}_2$ ase mimic **1** was achieved during 10 hours of irradiation with a maximum TOF of 50  $\text{H}_2$  per catalyst per hour. The result implies that both catalyst **1** and the MPA-CdTe species are regenerated and the whole reaction is photocatalytic in nature. The catalytic activity and stability are the highest known to date for iron catalytic reduction system for  $\text{H}_2$  production.<sup>[31]</sup>

To gain an insight into the photocatalytic  $\text{H}_2$  production from the aqueous solution, we studied the photophysical properties of the MPA-CdTe species with the addition of [FeFe]- $\text{H}_2$ ase catalyst **1**. The MPA-CdTe species exhibits broad absorption bands in a range of 350–670 nm (Figure S3). Excitation of the characteristic absorption of the MPA-CdTe species at 365 nm results in a maximal luminescence at 625 nm with a quantum yield of 0.458 based on quinine in 0.5 M  $\text{H}_2\text{SO}_4$  aqueous solution as the reference ( $\Phi = 0.546$ ).<sup>[32]</sup> The luminescence is very sensitive to the pH value of the solution. When the pH value of an aqueous solution of the MPA-CdTe was adjusted to 4.0–4.1 by HCl, the maximum of the luminescence shifted to lower energy at 675 nm with an accompanying decrease in luminescence intensity, lifetime, and quantum yield (Figure S4); these observations are consistent with those reported in the literature.<sup>[28,29]</sup> Progressive addition of [FeFe]- $\text{H}_2$ ase catalyst **1** into the solution of MPA-CdTe at pH 4.0 dramatically quenched the luminescence with a rate constant of  $1.43 \times 10^4 \text{ M}^{-1}$  (Figure 2 and Figure S5). Because of the small spectroscopic overlap of the absorption of [FeFe]- $\text{H}_2$ ase catalyst **1** and the emission of the MPA-CdTe species (Figure 2), the energy-transfer process from the excited MPA-CdTe species to [FeFe]- $\text{H}_2$ ase catalyst **1** would be negligible if it occurs. Therefore, the luminescence quenching of MPA-CdTe may be attributed to electron transfer from the excited MPA-CdTe species to [FeFe]- $\text{H}_2$ ase mimic **1**. To confirm this is indeed the case, we also estimated

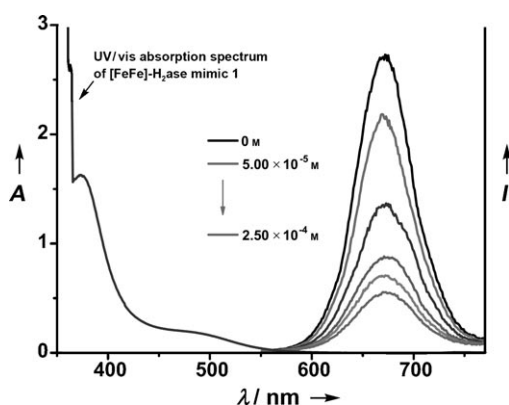


**Figure 2.** UV/Vis absorption spectrum of [FeFe]- $\text{H}_2$ ase mimic **1** ( $1.56 \times 10^{-4} \text{ M}$ ) in water and emission spectra of the MPA-CdTe ( $2.50 \times 10^{-4} \text{ M}$ ) at pH 4.0–4.1 in the absence and presence of [FeFe]- $\text{H}_2$ ase **1** ( $5.00 \times 10^{-5} \text{ M}$ – $2.50 \times 10^{-4} \text{ M}$ ), excited at 400 nm.

the free-energy change ( $\Delta G^0$ ) of this reaction. According to the valence-band energy level ( $E_{\text{vb}}$ ) of the thio-capped CdTe quantum dots ( $\approx 3.5 \text{ nm}$ ) which is 0.09 eV (all potentials discussed here are vs. NHE),<sup>[33]</sup> the reduction potential ( $E_{\text{red}}$ ) of [FeFe]- $\text{H}_2$ ase mimic **1** obtained from cyclic voltammograms is  $-0.88 \text{ eV}$  (Figure S6), the excited-state energy ( $E_{00}$ ) of the MPA-CdTe species is 1.98 eV at neutral pH and 1.84 eV at pH 4.0, respectively, the free-energy change ( $\Delta G^0$ ) was determined as  $-1.01 \text{ eV}$  at neutral pH and  $-0.87 \text{ eV}$  at pH 4.0. These findings indicate that the photoinduced electron-transfer process from the MPA-CdTe species to the catalytic centre **1** in this designed system is exothermic. Furthermore, the photoinduced electron-transfer process was evidenced by a flash photolysis study at room temperature. In the absence of [FeFe]- $\text{H}_2$ ase mimic **1**, no signal could be detected upon exposure to laser-pulsed light at 355 nm because the transient absorption of CdTe is too fast to be recorded by the time resolution of the instrument.<sup>[34]</sup> However, when [FeFe]- $\text{H}_2$ ase mimic **1** was introduced, three characteristic absorption bands at 420, 560, and 700 nm emerged immediately (Figure S7). These bands are quite similar to those of reported  $\text{Fe}^0\text{Fe}^{\text{I}}$  species generated by the reduction of a [FeFe]- $\text{H}_2$ ase mimic.<sup>[12,35]</sup> The decay throughout the absorption region occurred on the same time scale and could be well described by a monoexponential function with a lifetime of 278  $\mu\text{s}$  for the solution of the MPA-CdTe and [FeFe]- $\text{H}_2$ ase mimic **1**. Prolonged irradiation of the solution led to no permanent change, thus indicating the  $\text{Fe}^0\text{Fe}^{\text{I}}$  species formed by the photoinduced electron transfer was quite stable.

On the basis of the above results, it could be speculated that the excited MPA-CdTe species is oxidatively quenched by the [FeFe]- $\text{H}_2$ ase mimic **1** when irradiated by light, as simulated in Scheme 1. The reduced [FeFe]- $\text{H}_2$ ase mimic **1** can further react with a proton to afford  $\text{H}_2$  evolution.<sup>[36–39]</sup> On the other hand, the formed hole remaining in the MPA-CdTe species after electron transfer is subsequently regenerated by electron transfer from the sacrificial electron donor  $\text{H}_2\text{A}$ . It is known that the redox potential of  $\text{H}_2\text{A}$  is sufficiently negative to reduce the holes photogenerated in MPA-CdTe species,<sup>[23,40]</sup> but it is too positive to directly reduce [FeFe]- $\text{H}_2$ ase catalyst **1**. While the excited MPA-CdTe species is capable of both oxidative and reductive quenching with [FeFe]- $\text{H}_2$ ase catalyst **1** and  $\text{H}_2\text{A}$ , the relative extent of quenching and rate constants indicate that oxidative quenching with [FeFe]- $\text{H}_2$ ase catalyst **1** dominates (Figure S4). As compared with those reported in the literature,<sup>[11–21]</sup> the durability of the present system is greatly increased; possibly as a result of the stabilization of a catalytic intermediate that may relate to competitively oxidative and reductive quenching by [FeFe]- $\text{H}_2$ ase catalyst **1** and  $\text{H}_2\text{A}$ , respectively. Because two electrons are required to produce each molecule of  $\text{H}_2$ , the consecutive two-electron oxidation of  $\text{H}_2\text{A}$  is believed to be responsible for the regeneration of the MPA-CdTe species and [FeFe]- $\text{H}_2$ ase catalyst **1**.

In summary, a robust, inexpensive, and efficient photocatalytic system for  $\text{H}_2$  production from an artificial [FeFe]- $\text{H}_2$ ase mimic in an aqueous solution has been achieved. The TON (505) and TOF values ( $50 \text{ h}^{-1}$ ) obtained are competitive

with those from current state-of-the-art catalytic systems for  $H_2$  production. Although natural  $H_2$ ases have been incorporated with some semiconducting materials,<sup>[23,41,42]</sup> this is the first example of a synthetic [FeFe]- $H_2$ ase mimic combined with nanocrystal quantum dots for light-driven  $H_2$  evolution without any external manipulation.<sup>[43]</sup> We have shown that a synthetic [FeFe]- $H_2$ ase mimic, even the most popular one that would decompose generally on 1 hour irradiation, can be an effective catalyst for photochemical  $H_2$  production. The catalytic efficiency and stability indicate that both catalyst **1** and the MPA-CdTe species can be regenerated effectively during the entire photocatalytic reaction. Further studies on the mechanism are in progress to understand how the MPA-CdTe species associates with [FeFe]- $H_2$ ase mimic **1** and  $H_2A$ , and to improve the stability of [FeFe]- $H_2$ ase mimic and efficiency for light-driven  $H_2$  production.

### Experimental Section

All the experimental details were described in the Supporting Information. Characterization for [FeFe]- $H_2$ ase mimic **1**:  $^1H$  NMR (400 MHz,  $CD_3CN$ ):  $\delta$  = 7.86 (d,  $J$  = 7.5 Hz, 2H), 7.68 (s, 1H), 7.60 (d,  $J$  = 7.4 Hz, 4H), 7.40 (d,  $J$  = 7.3 Hz, 2H), 7.16 (s, 2H), 4.16 (d,  $J$  = 18.2 Hz, 6H), 3.80 (s, 4H), 3.71 (s, 2H), 3.63 (s, 6H), 3.54 (s, 12H), 3.45 (s, 10H), 3.27 (s, 9H), 2.11 (s, 2H), 1.81 (s, 4H), 1.27 ppm (s, 2H);  $^{13}C$  NMR (101 MHz,  $CDCl_3$ ):  $\delta$  = 211.03, 209.57, 170.78, 168.09, 166.88, 152.59, 141.62, 134.48, 132.86, 131.93, 129.58, 128.28, 127.40, 126.26, 125.74, 123.61, 107.70, 91.59, 90.10, 72.48, 72.03, 70.74, 70.62, 70.54, 69.88, 69.24, 59.10, 36.54, 36.26, 32.04, 30.64, 29.82, 29.48, 23.63, 22.82, 14.23 ppm; elemental analysis calcd for  $C_{55}H_{69}Fe_2N_3O_{19}S_2 \cdot 0.35CH_2Cl_2$ : C, 51.88; H, 5.48; N, 3.28; found: C, 51.88; H, 5.40; N, 3.38; IR ( $CH_2Cl_2$ ):  $\tilde{\nu}$  =  $\nu(CO)$  2039, 1998, 1970;  $\nu(C\equiv N)$  2284;  $\nu(C\equiv C)$  2123  $cm^{-1}$ ; ESIMS for **1**: two fragment peaks of **1**:  $m/z$  659.4 for [M1-H] and  $m/z$  663.4 for [M2] (Scheme S2).

A typical procedure for  $H_2$  production is as follows. Aqueous solution of [FeFe]- $H_2$ ase mimic **1** ( $3.12 \times 10^{-4} M$ ) and aqueous colloidal MPA-CdTe solution (5 mL,  $1.00 \times 10^{-3} M$ ) were added to a Schlenk tube. Different amount of ascorbic acid was dissolved in the mixed solution to obtain the desired concentration. The total volume of every sample was 10 mL. The pH value of the mixed solution was determined by a pH meter and was adjusted by the addition of aqueous NaOH or HCl solution. The sample was saturated by nitrogen gas to eliminate oxygen. Then  $CH_4$  (150  $\mu L$  in concentration effect and control experiments; 300  $\mu L$  in optimized concentration experiments to ensure enough  $CH_4$  was extracted from the samples) was injected as the internal standard for quantitative GC analysis. The sample was irradiated under a high-pressure Hanovia mercury lamp (500 W) with light wavelength longer than 400 nm. The generated photoproduct of  $H_2$  was characterized by GC analysis (14B Shimadzu) using nitrogen as the carrier gas with a molecular sieve column (5  $\text{\AA}$ ; 30 m  $\times$  0.53 mm) and a thermal conductivity detector. Then 200  $\mu L$  of mixed gas was extracted from the sample tube and injected into the GC. The response factor for  $H_2/CH_4$  was about 2.76 under the experimental conditions, which was established by calibration with known amounts of  $H_2$  and  $CH_4$ , and determined before and after a series of measurements.

Received: October 10, 2010

Revised: January 10, 2011

Published online: March 1, 2011

**Keywords:** artificial photosynthesis · electron transfer · hydrogen evolution · iron hydrogenases · photochemistry

- [1] H. B. Gray, *Nat. Chem.* **2009**, *1*, 7.
- [2] A. J. Esswein, D. G. Nocera, *Chem. Rev.* **2007**, *107*, 4022–4047.
- [3] M. Frey, *ChemBioChem* **2002**, *3*, 153–160.
- [4] M. W. W. Adams, E. I. Stiefel, *Science* **1998**, *282*, 1842–1843.
- [5] R. Cammack, *Nature* **1999**, *397*, 214–215.
- [6] D. Gust, T. A. Moore, A. L. Moore, *Acc. Chem. Res.* **2009**, *42*, 1890–1898.
- [7] A. Magnuson, M. Anderlund, O. Johansson, P. Lindblad, R. Lomoth, T. Polivka, S. Ott, K. Stensjö, S. Styring, V. Sundström, L. Hammarström, *Acc. Chem. Res.* **2009**, *42*, 1899–1909.
- [8] R. Lomoth, S. Ott, *Dalton Trans.* **2009**, 9952–9959.
- [9] W. Lubitz, E. J. Reijerse, J. Messinger, *Energy Environ. Sci.* **2008**, *1*, 15–31.
- [10] M. Wang, L. Sun, *ChemSusChem* **2010**, *3*, 551–554.
- [11] Y. Na, J. Pan, M. Wang, L. Sun, *Inorg. Chem.* **2007**, *46*, 3813–3815.
- [12] Y. Na, M. Wang, J. Pan, P. Zhang, B. Åkermark, L. Sun, *Inorg. Chem.* **2008**, *47*, 2805–2810.
- [13] D. Streich, Y. Astuti, M. Orlandi, L. Schwartz, R. Lomoth, L. Hammarström, S. Ott, *Chem. Eur. J.* **2010**, *16*, 60–63.
- [14] S. Ott, M. Kritikos, B. Åkermark, L. Sun, *Angew. Chem.* **2003**, *115*, 3407–3410; *Angew. Chem. Int. Ed.* **2003**, *42*, 3285–3288.
- [15] L.-C. Song, M.-Y. Tang, F.-H. Su, Q.-M. Hu, *Angew. Chem.* **2006**, *118*, 1148–1151; *Angew. Chem. Int. Ed.* **2006**, *45*, 1130–1133.
- [16] J. Ekström, M. Abrahamsson, C. Olson, J. Bergquist, F. B. Kaynak, L. Eriksson, L. Sun, H.-C. Becker, B. Åkermark, L. Hammarström, S. Ott, *Dalton Trans.* **2006**, 4599–4606.
- [17] W.-G. Wang, F. Wang, H.-Y. Wang, G. Si, C.-H. Tung, L.-Z. Wu, *Chem. Asian J.* **2010**, *5*, 1796–1803.
- [18] A. P. S. Samuel, D. T. Co, C. L. Stern, M. R. Wasielewski, *J. Am. Chem. Soc.* **2010**, *132*, 8813–8815.
- [19] X. Li, M. Wang, S. Zhang, J. Pan, Y. Na, J. Liu, B. Åkermark, L. Sun, *J. Phys. Chem. B* **2008**, *112*, 8198–8202.
- [20] A. M. Kluwer, R. Kapre, F. Hartl, M. Lutz, A. L. Spek, A. M. Brouwer, P. W. N. M. van Leeuwen, J. N. H. Reek, *Proc. Natl. Acad. Sci. USA* **2009**, *106*, 10460–10465.
- [21] H.-Y. Wang, W.-G. Wang, G. Si, F. Wang, C.-H. Tung, L.-Z. Wu, *Langmuir* **2010**, *26*, 9766–9771.
- [22] T. Nann, S. K. Ibrahim, P.-M. Woi, S. Xu, J. Ziegler, C. J. Pickett, *Angew. Chem.* **2010**, *122*, 1618–1622; *Angew. Chem. Int. Ed.* **2010**, *49*, 1574–1577.
- [23] K. A. Brown, S. Dayal, X. Ai, G. Rumbles, P. W. King, *J. Am. Chem. Soc.* **2010**, *132*, 9672–9680.
- [24] H. Zhang, Z. Zhou, B. Yang, *J. Phys. Chem. B* **2003**, *107*, 8–13.
- [25] L.-X. Shi, B. Hernandez, M. Selke, *J. Am. Chem. Soc.* **2006**, *128*, 6278–6279.
- [26] J. M. Tsay, M. Trzoss, L.-X. Shi, X. Kong, M. Selke, M. E. Jung, S. Weiss, *J. Am. Chem. Soc.* **2007**, *129*, 6865–6871.
- [27] W. W. Yu, L. Qu, W. Guo, X. Peng, *Chem. Mater.* **2003**, *15*, 2854–2860.
- [28] J. Aldana, N. Lavelle, Y. Wang, X. Peng, *J. Am. Chem. Soc.* **2005**, *127*, 2496–2504.
- [29] Y. Zhang, L. Mi, P.-N. Wang, J. Ma, J.-Y. Chen, *J. Lumin.* **2008**, *128*, 1948–1951.
- [30] J. Bhattacharyya, S. Das, S. Mukhopadhyay, *Dalton Trans.* **2007**, 1214–1220.
- [31] F. Gärtner, B. Sundararaju, A.-E. Surkus, A. Boddien, B. Loges, H. Junge, P. H. Dixneuf, M. Beller, *Angew. Chem.* **2009**, *121*, 10147–10150; *Angew. Chem. Int. Ed.* **2009**, *48*, 9962–9965.
- [32] C.-L. Wang, H. Zhang, J.-H. Zhang, N. Lv, M.-J. Li, H.-Z. Sun, B. Yang, *J. Phys. Chem. C* **2008**, *112*, 6330–6336.
- [33] T. Rajh, O. I. Mićić, A. J. Nozik, *J. Phys. Chem.* **1993**, *97*, 11999–12003.
- [34] S. Kaniyankandy, S. Rawalekar, S. Verma, D. K. Palit, H. N. Ghosh, *Phys. Chem. Chem. Phys.* **2010**, *12*, 4210–4216.

- [35] S. J. Borg, T. Behrsing, S. P. Best, M. Razavet, X. Liu, C. J. Pickett, *J. Am. Chem. Soc.* **2004**, *126*, 16988–16999.
  - [36] D. Chong, I. P. Georgakaki, R. Mejia-Rodriguez, J. Sanabria-Chinchilla, M. P. Soriaga, M. Y. Darensbourg, *Dalton Trans.* **2003**, 4158–4163.
  - [37] R. Mejia-Rodriguez, D. Chong, J. H. Reibenspies, M. P. Soriaga, M. Y. Darensbourg, *J. Am. Chem. Soc.* **2004**, *126*, 12004–12014.
  - [38] F. Gloaguen, J. D. Lawrence, T. B. Rauchfuss, *J. Am. Chem. Soc.* **2001**, *123*, 9476–9477.
  - [39] F. Gloaguen, T. B. Rauchfuss, *Chem. Soc. Rev.* **2009**, *38*, 100–108.
  - [40] H. Borsook, H. W. Davenport, C. E. P. Jeffreys, R. C. Warner, *J. Biol. Chem.* **1937**, *117*, 237–279.
  - [41] E. Reisner, J. C. Fontecilla-Camps, F. A. Armstrong, *Chem. Commun.* **2009**, 550–552.
  - [42] E. Reisner, D. J. Powell, C. Cavazza, J. C. Fontecilla-Camps, F. A. Armstrong, *J. Am. Chem. Soc.* **2009**, *131*, 18457–18466.
  - [43] L.-Z. Wu, F. Wang, X.-J. Wang, CN201010523037.4.
-